

Photoredox Behavior of Zinc(II) Porphyrins in Vesicle Assemblies

James K. Hurst,*[†] Lester Y. C. Lee,[†] and Michael Grätzel[‡]

Contribution from the Department of Chemistry and Biochemical Sciences, Oregon Graduate Center, Beaverton, Oregon 97006, and Institut de Chimie Physique, Ecole Polytechnique Fédérale, 1015 Lausanne, Switzerland. Received March 9, 1983

Abstract: Deactivation of photoexcited (5,10,15,20-tetrakis(*N*-methylpyridinium-4-yl)porphinato)zinc(II) ion (Zn(TMPyP)⁴⁺) adsorbed onto dihexadecyl phosphate (DHP) vesicles occurs by three kinetically well-resolved pathways. Reaction intermediates were identified from transient spectra. The rapidly ($t_{1/2} \sim 2 \mu\text{s}$) and slowly ($t_{1/2} \sim 200 \mu\text{s}$) decaying components are triplet ions, while the species decaying at the intermediate rate ($t_{1/2} \sim 20 \mu\text{s}$) are zinc(II) porphyrin π -cations and π -anions formed by charge transfer from a precursor whose lifetime is less than 100 ns. The relative proportion of triplet deactivation by the rapid pathway increased with increasing surface concentration of zinc(II) porphyrin, consistent with a concentration quenching mechanism. The π -ions and slowly decaying triplet are quenched by alkylviologens, which were also DHP bound. Quenching of the π -anion by *N*-methyl-*N'*-tetradecylbipyridinium (C₁₄MV²⁺) was shown to follow Stern-Volmer kinetics, with $k_Q = 1.7 \times 10^9 \text{ M}^{-1} \text{ s}^{-1}$ at 23 °C; quenching of the triplet ion was more complex, exhibiting apparent saturation at high surface viologen concentrations. Plausible reaction mechanisms are discussed within the framework of recently developed theories of reactions in microphase-separated media. The (5,10,15,20-tetrakis(4-sulfonatophenyl)porphinato)zinc(II) (Zn(TPPS)⁴⁺) triplet also undergoes bimolecular deactivation by DHP-bound alkylviologens: for C₁₄MV²⁺, $k_Q = 2.4 \times 10^8 \text{ M}^{-1} \text{ s}^{-1}$; for methylviologen (MV²⁺), $k_Q = 2.5 \times 10^9 \text{ M}^{-1} \text{ s}^{-1}$ at 23 °C. Oxidative quenching was confirmed by spectral detection of transitory viologen radical cations. When amine donors are present in solution, cyclic photosensitized redox transfer occurs with net formation of viologen radicals. When the oxidant ion, Fe(CN)₆³⁻, is incorporated within the vesicle inner aqueous phase, accumulation of reduced viologen is retarded in a manner suggesting that the viologens are capable of acting as transmembrane charge relays. Photoreactions of Zn(TMPyP)⁴⁺ ion with alkylviologens bound to lecithin liposomes are also briefly described.

Electron transport across biological membranes is an integral component of cellular energy storage. Respiration and photosynthesis occur in intricate assemblies of redox centers which have fairly precise topographic locations within the membrane matrices.¹ The question is presently unresolved whether this complexity is necessary to obtain efficient transmembrane electron transfer or, alternatively, is required for energy coupling,² e.g., proton translocation. Several reports of net oxidation-reduction across synthetic bilayer membranes have appeared for vesicles that contain only chlorophyll *a*,^{3,4} amphiphilic Zn(II) porphyrins,⁵ or amphiphilic Ru(bpy)₃²⁺ ions⁶ bound to both inner and outer surfaces; the conclusions drawn^{3,6} that redox occurs by rate-limiting electron exchange between sensitizer ions must be considered provisional.⁷ Various simple microheterogeneous systems that have been used to probe biological photophysics and photochemistry do not effectively mimic the behavior of photosynthetic membranes.⁸ Most strikingly, photosensitized reactions between membrane-bound redox components in the models are far less efficient than found in chloroplasts.^{9,10} Similarly, facile photosensitized redox reactions in homogeneous solution are often effectively quenched upon binding reactants to artificial vesicles^{11,12} (see, e.g., Figure 8). This conceptual problem of redox efficiencies is central to understanding membrane photobiology; its resolution may also yield fundamental insight into technical problems associated with development of artificial photoconversion and photostorage devices.¹³ For these reasons, we have sought to define the effects of membrane immobilization upon the photodynamic behavior of biological sensitizer molecules. The water-soluble Zn(II) porphyrins and various synthetic vesicles and alkylviologen dyes selected for these studies provide a convenient means for varying widely the spatial organization of reaction components.

Experimental Section

Reagents. Detailed procedures for preparation of DHP vesicle suspensions have been published.⁷ Formation of vesicles containing Fe(CN)₆³⁻ ion followed methods described for type II preparations except that 0.01–0.02 M K₃Fe(CN)₆ was added to the sonication mixture in place of methylviologen. Phosphatidylcholine vesicles were similarly

prepared by sonicating egg lecithin in an N₂ atmosphere for 2–3 h at 4 °C. The clarified solutions were then centrifuged at 100000g for 3 h. External ions were separated from vesicles by gel exclusion chromatography on a 1.6 × 40 cm Sephadex G-50 column. Lecithin was isolated from hen eggs by using methods described in the literature.¹⁴ Dihexadecyl phosphate (DHP) and methylviologen (MV²⁺) were recrystallized before use; other chemicals were reagent grade and used without further purification. Water was either doubly distilled or purified by reverse-osmosis ion-exchange chromatography. Photolysis solutions were purged of oxygen by slowly bubbling through the liquid a stream of nitrogen that had been passed over an activated copper bed; minimal purging times were about 45 min. *N*-Alkylviologens (C_{*n*}MV²⁺) and Zn(II) porphyrins used in these studies were the gifts of Drs. A. M. Braun and K. Kalyanasundaram, respectively, at EPFL, Lausanne.

Instrumental Methods. Flash kinetic studies were made by using the frequency-doubled pulse (532 nm, 15-ns width) from a JK 2000 Nd:YAG laser. Optical detection was essentially as previously described;¹⁵

- (1) See, e.g.: Haddock, B. A.; Jones, C. W. *Bacteriol. Rev.* **1977**, *41*, 47–99. Velthuys, B. R. *Annu. Rev. Plant Physiol.* **1980**, *31*, 545–567. Teide, D. M.; Leigh, J. S.; Dutton, P. L. *Biochim. Biophys. Acta* **1978**, *503*, 524–544.
- (2) Nicholls, D. G. "Bioenergetics"; Academic Press: New York, 1982.
- (3) Boyer, P. D.; Chance, B.; Ernster, L.; Mitchell, P.; Racker, E.; Slater, E. C. *Annu. Rev. Biochem.* **1977**, *46*, 955–1026.
- (4) Ford, W. E.; Tollin, G. *Photochem. Photobiol.* **1982**, *35*, 809–819.
- (5) Kurihara, K.; Sukigara, M.; Toyoshima, Y. *Biochim. Biophys. Acta* **1979**, *547*, 117–126.
- (6) Katagi, T.; Yamamura, T.; Saito, T.; Sasaki, Y. *Chem. Lett.* **1981**, 503–506, 1451–1454.
- (7) Laane, C.; Ford, W. E.; Otvos, J. W.; Calvin, M. *Proc. Natl. Acad. Sci. U.S.A.* **1981**, *78*, 2017–2020; Ford, W. E.; Otvos, J. W.; Calvin, M. *Ibid.* **1979**, *76*, 3590–3593.
- (8) Lee, L. Y.-C.; Hurst, J. K.; Politi, M.; Kurihara, K.; Fendler, J. H. *J. Am. Chem. Soc.* **1983**, *105*, 370–373.
- (9) Beddard, G. S.; Carlin, S. E.; Porter, G. *Chem. Phys. Lett.* **1976**, *43*, 27–32, and references therein.
- (10) Ilani, A.; Berns, D. S. *J. Membr. Biol.* **1972**, *8*, 333–356.
- (11) Kamen, M. "Primary Processes in Photosynthesis"; Academic Press: New York, 1963.
- (12) Kalyanasundaram, K.; Porter, G. *Proc. R. Soc. London, Ser. A* **1978**, *364*, 29–44.
- (13) Lee, L. Y. C. Ph.D. Dissertation, Oregon Graduate Center, 1983.
- (14) See, e.g.: Connolly, J. S., Ed. "Photochemical Conversion and Storage of Solar Energy"; Academic Press: New York, 1981, for leading references.
- (15) Barenholz, Y.; Gibbes, D.; Litman, B. J.; Goll, J.; Thompson, T. E.; Carlson, F. D. *Biochemistry* **1977**, *16*, 2806–2810.

[†]Oregon Graduate Center.
[‡]Ecole Polytechnique Fédérale.

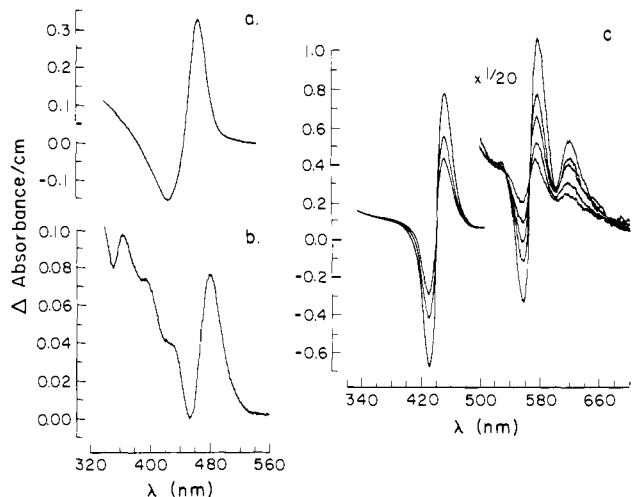


Figure 1. Optical difference spectra of DHP bound vs. unbound sensitizers. Curve a: 10 μM proflavin, 1.8 mM DHP vs. 10 μM proflavin in 0.1 M tricine, pH 7.2; curve b, 0.36 mM $\text{Ru}(\text{bpy})_3^{2+}$, 1.8 mM DHP vs. 0.36 mM $\text{Ru}(\text{bpy})_3^{2+}$ in 0.1 M tricine, pH 7.2; curve c, 1.6–9.5 μM $\text{Zn}(\text{TMPyP})^{4+}$, 2.4 mM DHP vs. 1.6–9.5 μM $\text{Zn}(\text{TMPyP})^{4+}$ in 0.05 M TEOA, pH 7.8. Spectra are uncorrected for scattering by DHP vesicles.

transient curves were recorded on a Tektronix WP-2221 data acquisition system equipped with R-7912 transient digitizers. Continuous photolysis experiments were carried out as previously described,⁷ except that for $\text{Zn}(\text{TPPS})^{4+}$ photoexcitation a Corning optical filter excluding light with wavelengths shorter than 495 nm was placed in the light beam. Optical absorption spectra were recorded on Cary Model 16 or Model 219 spectrophotometers. Light scattering measurements were made with a Chromatix KMX-6 photometer interfaced to a Langley-Ford autocorrelator. Turbidity was measured with a Hach 2100 A turbidimeter. Atomic absorption analysis was made in an air/acetylene flame with an Instrument Laboratories Model 254 spectrometer operated in the absorption mode. Ultrafiltration experiments were made in a 47-mm stirred cell by using Pellicon PSED semipermeable membranes with a nominal molecular weight cutoff of 2.5×10^4 amu; the cell was pressurized with N_2 gas to 20–25 psi.

Results and Discussion

Physical Properties of Vesicle-Containing Solutions. Synthetic anionic (DHP) and cationic dioctadecyldimethylammonium (DODAC) vesicles exhibit stability only over a relatively narrow range of solution conditions. In general, high salt concentrations¹⁶ or the presence of oxyanions or polyanions lead to destabilization. Thus, we were unable to form DODAC vesicles by sonication in solutions containing phosphate, sulfate, or dithionite ions, or in EDTA-containing buffers when $\text{pH} > 5$, or to form DHP vesicles in acidic media ($\text{pH} < 6$), or in solutions containing high concentrations of glycine (0.1 M), ferricyanide (0.05 M), EDTA (0.3 M), tetramethylammonium (0.5 M), or acetate (0.1 M) ions. However, several amines possessing hydroxylic substituents as a common structural feature (tricine, triethanolamine (TEOA), tris(hydroxymethyl)aminomethane (Tris)) were found to dramatically enhance both vesicle formation and longevity. DHP vesicles formed in these buffers had somewhat smaller hydrodynamic radii⁷ (~ 500 Å) than vesicles in pure H_2O (600 Å),¹⁷ as measured by quasielastic light-scattering spectroscopy.¹⁸ Concentrations of TEOA in excess of 0.25 M were found to displace bound $\text{Zn}(\text{TMPyP})^{4+}$ ion from DHP (discussed below); optical difference spectra gave no evidence of possible TEOA ligation to the metal. Displacement is not due to simple salt effects, since tetramethylammonium chloride at comparable ionic strength (≤ 0.5 M) had no detectable effect on binding. Vesicle sizes are unaltered by TEOA concentrations as high as 1 M. Other researchers have

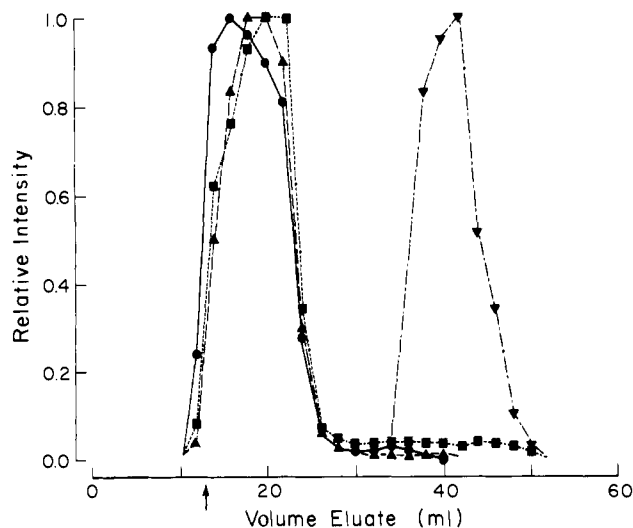


Figure 2. Chromatography of DHP vesicles containing adsorbed $\text{Zn}(\text{TMPyP})^{4+}$ and $\text{C}_{14}\text{MV}^{2+}$ ions on Sephadex G-50 dextran gels. A sample of 2.4 mM DHP sonicated in the presence of 0.5 mM $\text{C}_{14}\text{MV}^{2+}$ and 20 μM $\text{Zn}(\text{TMPyP})^{4+}$ in 0.02 M Tris, pH 7.8. Solid line, relative turbidity; dashed line, zinc(II) porphyrin absorption, measured at 446 nm; dotted line, viologen, measured as the $\text{C}_{14}\text{MV}^{2+}$ radical ion at 560 nm by $\text{Na}_2\text{S}_2\text{O}_4$ addition⁷ to eluate fractions; alternate dash-dotted line, viologen peak obtained in the absence of DHP vesicles. The arrow indicates column void volume determined with blue dextran.

found that 0.05 M Tris severely limits the extent of adsorption of $\text{Ru}(\text{bpy})_3^{2+}$ ion by DHP.¹⁹ These observations suggest that the amines are acting as stabilizing cosurfactants by direct adsorption at the vesicle interface. Liposomes formed from zwitterionic phosphatidylcholine esters are far less sensitive to the presence of various ionic solutes.

Binding of chromophoric dyes to vesicle surfaces gives rise to observable shifts in their optical spectra. Several examples are given in Figure 1. For $\text{Zn}(\text{TMPyP})^{4+}$ ion,²⁰ strong binding to DHP was confirmed by membrane ultrafiltration and gel chromatography experiments. Specifically, addition of DHP vesicles to solutions containing $\text{Zn}(\text{TMPyP})^{4+}$ ion completely blocks its passage through semipermeable membranes that exclude the vesicles; the ion passes freely when vesicles are absent. The metalloporphyrin also cochromatographs with the vesicles on molecular sieving gels (Bio-Gel P-2, Sephadex G-50) under conditions where unbound $\text{Zn}(\text{TMPyP})^{4+}$ is significantly retarded (Figure 2). Dyes that do not bind show no spectral perturbation. Thus, addition of $\text{Zn}(\text{TPPS})^{4+}$ to DHP vesicles or $\text{Zn}(\text{TMPyP})^{4+}$ ion to phosphatidylcholine liposomes gave neither detectable optical difference spectra nor retardation of the metalloporphyrin by ultrafiltration.

Optical difference spectra obtained by titrimetric addition of $\text{Zn}(\text{TMPyP})^{4+}$ to DHP vesicles obeyed Beer's law over the measured concentration range [$\text{Zn}(\text{TMPyP})^{4+}$] = 1.6–210 μM ; this observation indicates essentially complete metalloporphyrin binding to the vesicle under these experimental conditions. Spectral band shapes were constant, with difference spectra showing isosbestic points at 433, 540, and 566 nm.⁷ Spectral curves obtained by direct comparison of solutions containing varying ratios (r) of DHP bound $\text{Zn}(\text{TMPyP})^{4+}$ ([DHP] = 4.9 mM, [$\text{Zn}(\text{TMPyP})^{4+}$] = 5.3 μM , $r = 824$, vs. [DHP] = 1.2 mM, [$\text{Zn}(\text{TMPyP})^{4+}$] = 27 μM , $r = 44$) were also identical. These results indicate that chromophore adsorption is unchanged by varying the extent of particle loading. No evidence exists, therefore, to suggest binding-site heterogeneity or heme aggregation, which would be anticipated to cause peak broadening

(15) McNeil, R.; Richards, J. T.; Thomas, J. K. *J. Phys. Chem.* **1970**, *74*, 2290–2294.

(16) Mortara, R. A.; Quina, F. H.; Chaimovich, H. *Biochem. Biophys. Res. Commun.* **1978**, *81*, 1080–1086.

(17) Hermann, U.; Fendler, J. H. *Chem. Phys. Lett.* **1979**, *64*, 270–274.

(18) Berne, B. J.; Pecora, R. "Dynamic Light Scattering"; Wiley-Interscience: New York, 1976.

(19) Tricot, Y.-M.; Furlong, D. N.; Sasse, W. H. F.; Davis, P.; Snook, I. *Aust. J. Chem.* **1983**, *36*, 609–612.

(20) Abbreviations used: $\text{Zn}(\text{TMPyP})^{4+}$, 5,10,15,20-tetrakis(*N*-methylpyridinium-4-yl)porphyrinatozinc(II); $\text{Zn}(\text{TPPS})^{4+}$, (5,10,15,20-tetrakis(4-sulfonatophenyl)porphyrinato)zinc(II); C_nMV^{2+} (alkylviologen), *N*-methyl-*N*-alkyl-4,4'-bipyridinium.

accompanied by slight shifts in maximal positions.^{21,22} Absorption band maxima of Zn(TMPyP)⁴⁺ dissolved in various organic solvents showed a progressive red shifting with decreasing solvent polarity. The spectrum of DHP-bound Zn(TMPyP)⁴⁺ matched fairly well that obtained in the less polar alcohols, e.g., 2-propanol, which is consistent with binding in the region of the polar head-groups on the vesicle surface.

Binding of methylviologen and various alkylviologen cations to DHP vesicles was demonstrated by their comigration on dextran gels under conditions where unbound viologens exhibit considerably greater retention times (Figure 2). Similarly, C₁₆MV²⁺²⁰ was found to comigrate with lecithin liposomes in 0.05 M phosphate buffer, pH 6.5, although for solutions containing liposomes and C₁₄MV²⁺, a minor fraction (~25%) of the viologen was observed to elute well after the C₁₄MV²⁺ liposome particle, indicating incomplete binding by the shorter chain alkylviologen. Careful scrutiny of the elution profiles obtained for both DHP vesicles and liposomes suggests that the distribution of adsorbed ions increases in successive fractions taken across the band (Figure 2). This apparent concentration heterogeneity might be the consequence of dynamic equilibria between predominantly bound and a small amount of unbound ions, such that ions are lost from vesicles on the leading edge of the band during passage down the column to be scavenged by following vesicles, which thereby become more concentrated. Alkylviologen radicals formed by one-electron reduction apparently remain bound to the vesicles. Electronic spectra show the appearance of a strong sharp band at 395 nm and a broad absorption envelope throughout the visible region centered at 602 nm, diagnostic of the blue monomeric species; in contrast, alkylviologen monocation radicals in homogeneous solution exhibit broad absorption bands at 382 and 545 nm characteristic of purple multimeric forms.²³ Aggregation is therefore precluded in vesicle suspensions, presumably by vesicle binding. Adsorption of Zn(TMPyP)⁴⁺ and/or MV²⁺ or C₁₄MV²⁺ onto DHP vesicles had no measurable effect upon the hydrodynamic radii or size distributions of the particles.⁷ Binding of C₁₄MV²⁺ ion (0.71 mM) to Zn(TMPyP)⁴⁺-DHP particles ([Zn(TMPyP)⁴⁺] = 21 μM, *r* = 114) caused no significant chromophoric perturbation.

Asymmetric DHP vesicles containing ferricyanide occluded within their inner aqueous phase were prepared by sonication in aqueous buffer (0.02 M Tris, pH 7.8) containing 0.02 M Fe(CN)₆³⁻ ion and then passed down a Sephadex G-50 column. Absence of Fe(CN)₆³⁻ in the external solution was confirmed by analyzing eluate fractions from membrane ultrafiltration by atomic absorption spectroscopy. Whether analysis was made immediately or several hours after isolation, the iron content in the external medium was below detectable limits (0.3 μM). In contrast, solutions containing the membrane-impermeable vesicles gave apparent Fe(CN)₆³⁻ concentration levels of 4–40 μM, depending upon the vesicle concentrations.²⁴ At the higher concentrations,

(21) Pasternack, R. F.; Francesconi, L.; Raff, D.; Spiro, E. *Inorg. Chem.* **1973**, *12*, 2606–2611.

(22) White, W. I., in "The Porphyrins"; Dolphin, D., Ed.; Academic Press: New York, 1978; Vol. V, Chapter 7.

(23) Monserrat, K.; Grätzel, M. *J. Chem. Soc., Chem. Commun.* **1981**, 183–184.

(24) Assuming spherical symmetry, with a particle radius of 240 Å, bilayer width of 50 Å, and DHP monomer surface area of 70 Å², we calculate that each vesicle contains ~17 000 surfactant molecules. When [DHP] = 6–30 mM, the vesicle concentrations are about 0.35–1.8 μM and the occluded volume is 0.6–3.1% of the total solution volume. The maximal ferricyanide incorporation within the inner aqueous microphase when DHP is sonicated in 0.02 M Fe(CN)₆³⁻ should then give an apparent solution concentration of 0.12–0.6 mM, which is an order of magnitude greater than experimentally measured. Recent detailed²⁵ analyses of the light-scattering properties of DHP vesicles suggest a bimodal distribution of sizes, for which the minor fraction (1–2%) of strongly scattering large vesicles drastically increases the apparent hydrodynamic radii of the major component. When corrected for this effect, the average radius of the major fraction is calculated to be about 150 Å. This size is consistent with radii (200–250 Å) determined by electron microscopy.^{16,26} Apparent solution concentrations of Fe(CN)₆³⁻ based upon a 150-Å radius are 0.05–0.26 mM. These values are in better agreement with experimentally measured concentration levels, although still severalfold higher, suggesting either that the particles are not spherically symmetrical or that Fe(CN)₆³⁻ is partially excluded from the vesicle interior.

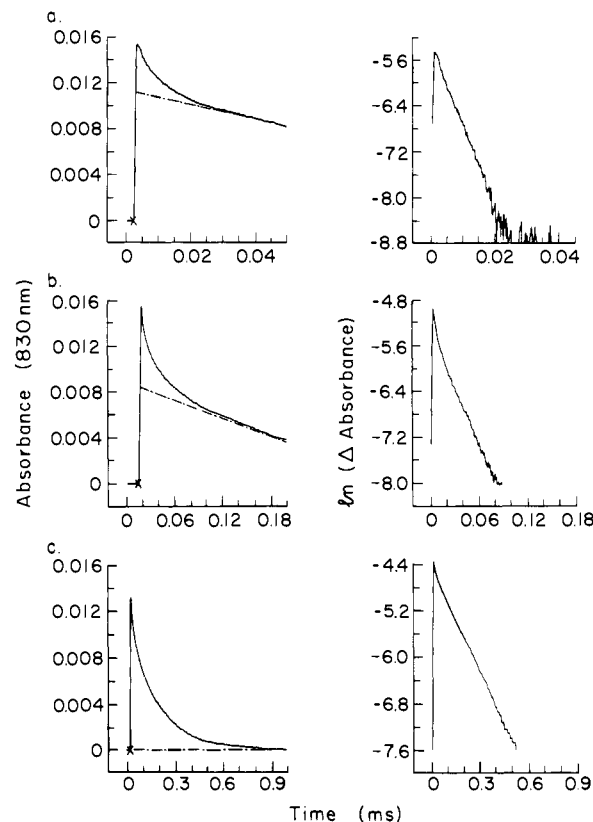


Figure 3. Deactivation of photoexcited Zn(TMPyP)⁴⁺-DHP particles. Left column, curves a–c, time course of absorbance changes following 532-nm laser flash excitation (marked with an X); right column, curves a–c, kinetic analysis assuming three concurrent first-order reactions, using estimated baselines shown for curves a and b. Reaction conditions: 10 μM Zn(TMPyP)⁴⁺, 6 mM DHP in 0.02 M Tris, pH 7.8, at 23 °C.

Fe(CN)₆³⁻ could also be detected by optical spectroscopy. Difference spectral curves of the Fe(CN)₆³⁻ containing vesicles against similar vesicles prepared in the absence of ferricyanide gave an absorption band at 420 nm ascribable to the ion. From its molar absorptivity ($\epsilon_{420} = 1040 \text{ M}^{-1} \text{ cm}^{-1}$) apparent Fe(CN)₆³⁻ concentrations were calculated that agreed with the atomic absorption results. These experiments demonstrate that Fe(CN)₆³⁻ ions are incorporated within the DHP vesicles, that clean chromatographic separation from the ions in the external medium has been made, and that passive diffusion of the ions across the bilayer is negligible over the time span of the photolysis experiments described below.

We have recently discovered that diffusion of MV²⁺ contained within DHP vesicles is dramatically enhanced in the presence of light by redox photosensitizing dyes bound to the vesicle surface.⁷ This photostimulated diffusion is not expected to occur in instances where the chromophore does not bind to the vesicle. To examine this point, we sought evidence for Fe(CN)₆³⁻ leakage from an asymmetrically organized system comprising DHP vesicles with C₁₆MV²⁺ bound to both surfaces, Fe(CN)₆³⁻ ion within the inner aqueous phase, and Zn(TPPS)⁴⁺ ion in the external phase. The buffered solution, pH 7.8, contained 0.02 M Tris and 0.1 M tricine, the latter acting as sacrificial donor. Illumination with visible light ($\lambda > 500 \text{ nm}$) gave rise to C₁₆MV⁺ radical cation formation as described below. After 60 min, the distribution of Fe(CN)₆³⁻ in the aqueous phases was determined by membrane ultrafiltration and atomic absorption analysis. As before, no iron was detectable in vesicle-free fractions, and the concentration level determined in the vesicle-containing solution was unchanged from the value measured before illumination. Therefore, in these systems, photoexcitation and oxidative quenching of Zn(TPPS)⁴⁺ by viologen acceptors bound to the vesicle do not induce transmem-

(25) Tricot, Y.-M.; Furlong, D. N.; Sasse, W. H. F.; Daivis, P.; Snook, I.; van Megan, W., manuscript in preparation.

(26) Lukac, S. *Photochem. Photobiol.* **1982**, *36*, 13–20.

Table I. Physical Characteristics of Zn(TMPyP)⁴⁺-DHP Vesicles^a

[DHP] ^b	% surface coverage ^c	mean P...P distance, Å ^d	³ (Zn(TMPyP) ⁴⁺) deactivation	
[Zn(TMPyP) ⁴⁺]			<i>k</i> , s ⁻¹	initial absorbance ^e
600	0.24	231	<i>k</i> ₁ = 1.5 × 10 ⁵ <i>k</i> ₂ = 3.1 × 10 ⁴ <i>k</i> ₃ = 5.6 × 10 ³	<i>A</i> ¹ = 0.047 <i>A</i> ² = 0.046 <i>A</i> ³ = 0.112
120	1.2	103	<i>k</i> ₁ = 3.4 × 10 ⁵ <i>k</i> ₂ = 3.5 × 10 ⁴ <i>k</i> ₃ = 1.9 × 10 ³	<i>A</i> ¹ = 0.107 <i>A</i> ² = 0.051 <i>A</i> ³ = 0.034
30	4.8	52	<i>k</i> ₁ = 3.9 × 10 ⁵ <i>k</i> ₂ = 4.1 × 10 ⁴ <i>k</i> ₃ = 4.7 × 10 ³	<i>A</i> ¹ = 0.154 <i>A</i> ² = 0.071 <i>A</i> ³ = 0.047

^a In 0.02 M Tris, pH 7.8, 23 °C. ^b [Zn(TMPyP)⁴⁺] = 10–40 μM; [DHP] = 1.2–6.0 mM. ^c Calculated by assuming 70 and 100 Å² for DHP monomer and Zn(TMPyP)⁴⁺ surface areas, respectively. ^d Center-to-center distance. ^e Absorbances at 830 nm of transient species decaying by each pathway extrapolated to initial time.

brane diffusion of Fe(CN)₆³⁻ located within the vesicle.

Deactivation of Zn(II) Porphyrin Photoexcited States. Photoexcited Zn(TMPyP)⁴⁺ ion underwent exponential decay in dilute (5–20 μM) aqueous solutions; lifetimes varied slightly in differing buffer systems (τ = 100–222 μs), presumably because contributions from impurity quenching differed,²⁷ but were similar to previously reported values for triplet deactivation.^{28,29} Both Zn(TMPyP)⁴⁺ in solutions containing egg lecithin liposomes and Zn(TPPS)⁴⁺ in anionic DHP vesicle suspensions gave single exponential relaxation curves (τ = 254 μs, 71 μs, respectively) when photoexcited. As discussed above, the Zn(II) porphyrins do not adsorb to vesicles in these systems. At these concentration levels ([Zn(TMPyP)⁴⁺] ≈ 10 μM), bimolecular deactivation by T–T annihilation or ground-state quenching is not significant.³⁰

Complex multicomponent deactivation is observed to follow photoexcitation of DHP-bound Zn(TMPyP)⁴⁺ ion. There appear to be three distinct steps that occur on time scales that are separable by about an order of magnitude (Figure 3). The minimal kinetic scheme that can account quantitatively for the curves requires use of three concurrent first-order relaxation processes. It is difficult to determine reaction order from curve fitting the integrated rate law, however, since combinations of first-order and second-order processes also reproduce the curves fairly well. Biphotonic excitation does not contribute to the kinetic complexity since relative amplitudes of the three deactivation pathways are independent of laser flash intensity over a 25-fold range. Under these conditions the *total* amplitudinal change is seen to vary about 4-fold, reflecting differences in concentrations of initially photoexcited Zn(II) porphyrins. Nearly identical behavior was seen for vesicle suspensions containing Zn(TMPyP)⁴⁺ ion bound to both inner and outer surfaces and bound only externally, so the various pathways cannot be associated with vesicle "sidedness", i.e., geometrical constraints arising from differing packing forces on the concave and convex surfaces. First-order rate constants for each decay component appeared to be independent of pulse intensity, although this conclusion is relatively uncertain for the intermediate pathway since corrections for the faster and more slowly decaying components could generate a relatively large computational error as determined by the extrapolative method outlined in Figure 3. Relative amplitudes of the various steps were sensitive to the extent of sensitizer binding to the vesicle. As surface coverage increased progressively from about 28 Zn(TMPyP)⁴⁺/vesicle to 570 Zn(TMPyP)⁴⁺/vesicle, the amplitude of the fast-decaying component increased about 3-fold at the expense of the slowly decaying component, while the amplitude

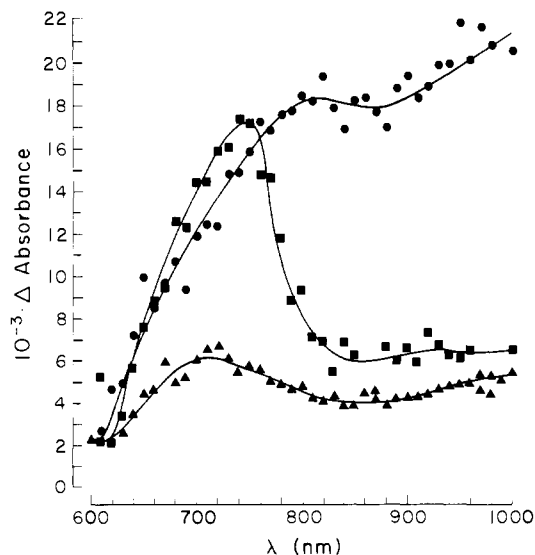


Figure 4. Spectra of Zn(TMPyP)⁴⁺-DHP photoexcitation intermediates. End-of-pulse spectra for rapid (circles), intermediate (squares) and slowly decaying components (triangles) of triphasic deactivation curves calculated from transient spectra at 1.5, 4.8, 16, 50, and 230 μs after excitation. Reaction conditions: 20 μM Zn(TMPyP)⁴⁺, 2.4 mM DHP in 0.02 M Tris, pH 7.8, at 23 °C.

of the component decaying at the intermediate rate remained relative constant (Table I). Measured rate constants for the fast component also appeared to increase somewhat with increasing sensitizer concentration under these conditions, with *k*₁ = (1.5–3.9) × 10⁵ s⁻¹ at the limiting concentrations. Rate constants for intermediate (*k*₂ = (3–4) × 10⁴ s⁻¹) and slowly decaying components (*k*₃ = (2–5) × 10³ s⁻¹) showed no systematic variation with sensitizer concentration; the relatively wide range of values for the latter can probably be attributed to differing levels of impurity quenching in different samples.²⁷ Rate constants were independent of detection wavelength over the range investigated (700–890 nm).

The conclusion drawn from the kinetic analysis that there are three distinct deactivation pathways is supported by the transient spectral properties. We have plotted in Figure 4 the spectra of the absorbing species, which are determined from spectra taken at various times after the laser flash. Briefly, the method involves calculating the relative concentrations of each component contributing to the spectra from the measured first-order rate constants and then solving simultaneous equations to obtain spectra of the pure components. Amplitudes recorded in Figure 4 therefore correspond to end-of-pulse spectra, i.e., before the onset of kinetic decay. Both fast and slowly reacting species exhibit broad absorption envelopes throughout the near-IR region that are nearly identical with the spectrum reported for the triplet-excited Zn(TMPyP)⁴⁺ ion in solution.³¹ The broad maximum centered at 740 nm in the spectrum of the other component suggests the predominance of metalloporphyrin π-cations and π-anions. Both ions exhibit strong absorption bands in this region in aqueous solution (Zn(TMPyP)⁵⁺, $\epsilon_{700} \approx 0.9 \times 10^4$ M⁻¹ cm⁻¹; Zn(TMPyP)³⁺, $\epsilon_{710} \approx 1.6 \times 10^4$ M⁻¹ cm⁻¹);^{32,33} the apparent bathochromic shift evident in the transient spectrum might be a consequence of adsorption onto DHP. Ionogenic photochemical reactions have been reported for several other metalloporphyrins in homogeneous solution.^{34,35} In these instances, the π-ions are formed by electron transfer between two triplet-state porphyrins and/or a triplet- and ground-state porphyrin. From examination

(27) McCartin, P. J. *Trans. Faraday Soc.* **1964**, *60*, 1694–1701.

(28) Kalyanasundaram, K.; Grätzel, M. *Helv. Chim. Acta* **1980**, *63*, 478–485.

(29) Harriman, A.; Porter, G.; Richoux, M.-C. *J. Chem. Soc., Faraday Trans. 2* **1981**, *77*, 833–844.

(30) Pekkarinen, L.; Linschitz, H. *J. Am. Chem. Soc.* **1960**, *82*, 2407–2411.

(31) Kalyanasundaram, K.; Neumann-Spallart, M. *J. Phys. Chem.* **1982**, *86*, 5163–5169.

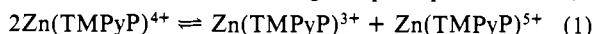
(32) Neta, P. *J. Phys. Chem.* **1981**, *85*, 3678–3684.

(33) Borgarello, E.; Kalyanasundaram, K.; Okuno, Y.; Grätzel, M. *Helv. Chim. Acta* **1981**, *64*, 1937–1942.

(34) Ballard, S. G.; Mauzerall, D. C. *J. Chem. Phys.* **1980**, *72*, 933–947.

(35) Carapellucci, P. A.; Mauzerall, D. *Ann. N.Y. Acad. Sci.* **1975**, *244*, 214–238.

of the transient spectra obtained for Zn(TMPyP)⁴⁺/DHP vesicles it appears that the ions are not formed from the fast-decaying triplet component. If this were so, one would expect to see dramatic distortion of the triplet spectrum since it must then be the difference between triplet and π -ion absorptions. It is possible that another, yet more rapidly decaying, triplet is the precursor of the electron-transfer products, although we were unable to detect such a component in the pulsed laser experiments. Alternatively, charge transfer could occur directly from the initially photoexcited singlet state. Ionogenesis according to eq 1 requires 2.03 eV:³¹



the Zn(TMPyP)⁴⁺ excited singlet and triplet states lie at 2.0 and 1.6 eV above the ground state, respectively.^{29,31} Electron transfer might occur between two photoexcited ions or from higher photoexcited states reached by two-photon absorption. However, since there is no evidence that the relative yields of π -ions initially formed increase disproportionately with increasing laser flash intensity, these pathways apparently make insignificant contributions to the overall reaction. From reported molar absorptivities measured in solution,³¹⁻³³ we calculate that about 3×10^{-7} M of each of the Zn(II) π -ions and 4×10^{-6} M triplet ions are formed in the laser flash under conditions given in Figure 4. Overall, then, less than 25% of the porphyrin is initially photoexcited, which is also consistent with the notion that T-T annihilation or two-photon reactions are unimportant. Energetic considerations would therefore seem to require that electron transfer occur directly from the photoexcited singlet state since reaction from the triplet state is endergonic by about 400 mV. However, Ballard and Mauzerall have observed zinc(II) octaethylporphyrin π -ion formation from the photoexcited triplet state in the face of energetic constraints quite similar to this system.³⁴ They argue that conclusions regarding triplet-state reactivities based upon electrochemical potentials fail to take proper account of entropy effects and, more generally, that quasithermodynamic models are inherently incapable of quantitatively describing very rapid reactions. Conclusive identification of the ionogenic photoexcited state of the Zn(TMPyP)⁴⁺ ion will probably require direct examination of the kinetic behavior of the Zn(II) porphyrin excited singlet state.

Redox Quenching of Photoexcited Zn(II) Porphyrins

Reduction Reactions. Triethanolamine and tricine act as donors in photocatalytic reduction of the viologens by Zn(TMPyP)⁴⁺ ion. Under continuous illumination TEOA is severalfold more effective in promoting C₁₄MV²⁺ reduction, both in the presence and in the absence of DHP vesicles. Reductive quenching of the Zn(TMPyP)⁴⁺ triplet ion in solution is observed at high TEOA concentrations. The reaction follows Stern-Volmer kinetics, with $k_Q = 4 \times 10^3 \text{ M}^{-1} \text{ s}^{-1}$ ([TEOA] = 0.05–1.0 M, pH 7.8, $\mu = 0.50$ (Me₄NCl), 23 °C). Quenching by TEOA is therefore inefficient; by comparison, for EDTA, $k_Q = 1.7 \times 10^5 \text{ M}^{-1} \text{ s}^{-1}$ at 23 °C, $\mu = 0.05$ M.²⁹ The transient absorption spectrum of photoredox products observed 2 ms after pulse shows weak absorption throughout the 600–900-nm region, with a peak maximum around 640 nm. The spectral characteristics do not correspond to the Zn(II) porphyrin π -anion, but may be due to dihydroporphyrin formed by its disproportionation.³⁶ A similar band has been observed to form upon continuous illumination of Zn(TMPyP)⁴⁺ in the presence of EDTA.²⁸

Reductive quenching of DHP-bound Zn(TMPyP)⁴⁺ by TEOA could not be measured. The triphasic relaxation curves were unaffected by addition of low TEOA concentration levels (≤ 0.05 M). At higher TEOA (≥ 0.25 M), the faster decaying components were lost with collapse to a single exponential decay appearing on the millisecond time scale. Coincident with these kinetic changes, the Zn(TMPyP)⁴⁺ optical spectrum underwent a hypsochromic shift to that of the unbound ion and DHP vesicles lost their capability of preventing Zn(TMPyP)⁴⁺ ion diffusion across semipermeable membranes. These studies clearly demonstrate the displacement of Zn(TMPyP)⁴⁺ from DHP by high concen-

tration levels of TEOA. Evidence indicating that some sensitizer photoreduction occurs in Zn(TMPyP)⁴⁺-DHP vesicles at low TEOA concentration levels was the observation of an absorbing product in the 600–700-nm region following laser flash excitation. Also, the Zn(II) porphyrin spectrum slowly bleaches after having once been exposed to the light beam, going colorless after several hours. These dark reactions did not require DHP and did not occur in the absence of donor amines (e.g., negligible bleaching was obsd. in 0.02 M glycine, pH 8.0, that had been repeatedly exposed to laser pulses) or in the presence of these amines (TEOA, tricine) when protected from the light. These changes undoubtedly reflect continued reduction of the porphyrins by further reactions with the immediate amine oxidation products and/or disproportionation of initially formed dihydroporphyrins.^{37,38} Sensitizer bleaching was also observed during continuous illumination in systems containing TEOA, Zn(TMPyP)⁴⁺, and viologen acceptors. The bleaching reaction(s) were inversely dependent upon acidity and could be prevented in homogeneous solution by maintaining slightly alkaline conditions. However, photoreduction of DHP-bound sensitizer was extensive in neutral media, giving rise to 50% bleaching after several hours of exposure in typical cases. Presumably, this instability reflects the greater acidity present at the aqueous anionic vesicle interface. The rate of bleaching increases with increasing Zn(II) porphyrin/DHP ratios, consistent with the notion that photoreduction is initiated by π -anion disproportionation and hence increases proportionately with reactant surface concentration. Reductive quenching of the Zn(TMPyP)⁴⁺ triplet followed first-order kinetics in solutions containing lecithin vesicles; the decay rate increased 4-fold upon adding 1 mM EDTA to the suspensions in 0.05 M phosphate buffer, pH 6.5. This rate increase is higher than anticipated, based upon previously reported quenching constants under other conditions;^{28,29} direct comparison is difficult since the reaction rate is sensitive to both ionic strength and acidity.

Oxidative Quenching by Viologens. The triplet-excited Zn(TMPyP)⁴⁺ ion has been shown to undergo one-electron oxidation by MV²⁺, with $k_Q = 1.8 \times 10^7 \text{ M}^{-1} \text{ s}^{-1}$ at 23 °C in phthalate buffer, pH 5.0, $\mu = 0.05$ (NaCl).²⁹ On the basis of a limited data set, we find for quenching by C₁₄MV²⁺ $k_Q = 5.3 \times 10^7 \text{ M}^{-1} \text{ s}^{-1}$, in 0.05 M TEOA, pH 7.8, at 23 °C. Viologen radical formation is suggested by the appearance of an absorbing species below 700 nm, which forms at a rate identical with triplet-state deactivation. The effect is particularly clear at 580 nm where ground-state and triplet ion spectra are isosbestic.³¹ Under the experimental conditions, reductive quenching should not contribute significantly to the overall deactivation process. Consistent with this expectation, we find the level of transitory near-IR absorption ($\lambda > 700$ nm) is nearly abolished and photolytic bleaching of Zn(TMPyP)⁴⁺ is retarded by C₁₄MV²⁺ addition. Similar protective action by MV²⁺ has previously been noted for solutions containing EDTA and Zn(TMPyP)⁴⁺ ion.^{28,29}

Deactivation rates corresponding to the intermediate and slow pathways in photoexcited Zn(TMPyP)⁴⁺-DHP particles increase upon adding C₁₄MV²⁺ to the vesicle suspensions; the rate of the rapidly decaying component is unaffected by concentration levels up to 1 mM. Bimolecular quenching was observed for the intermediate pathway, with $k_Q = 1.7 \times 10^9 \text{ M}^{-1} \text{ s}^{-1}$ in 0.02 M Tris, pH 7.8 at 23 °C; reaction of the slowly decaying component appears more complex (Figure 5). Quantitative study of the two quenching reactions was made at low ($r = 60$) and high ($r = 600$) DHP/Zn(TMPyP)⁴⁺ ratios to enhance the extent of reaction by intermediate and slow pathways, respectively. There was no evidence of static quenching, e.g., that might arise by aggregation of bound Zn(TMPyP)⁴⁺ and C₁₄MV²⁺ ions; initial amplitudes for the various steps were unchanged by addition of the viologen. Spectra of the slowly decaying component and two rapidly decaying components were calculated from transient spectra taken at 1.0 and 50 μs after pulse by the method previously described. The spectral changes (Figure 6) demonstrate rapid loss of the

(36) Seely, G. R.; Calvin, M. *J. Chem. Phys.* **1955**, *23*, 1068–1078. Seely, G. R.; Talmadge, K. *Photochem. Photobiol.* **1964**, *3*, 195–206.

(37) Mauzerall, D. *J. Am. Chem. Soc.* **1962**, *84*, 2437–2445.

(38) Mauzerall, D., in ref 22, pp 45–46.

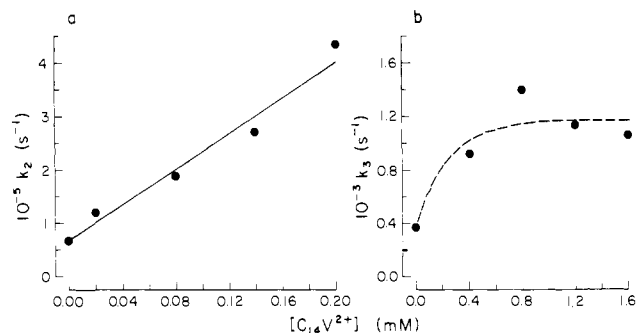


Figure 5. $C_{14}MV^{2+}$ quenching of $Zn(TMPyP)^{4+}$ -DHP photoexcitation intermediates. Graph a, viologen dependence for π -ion quenching, measured at 770 nm, with 20 μM $Zn(TMPyP)^{4+}$, 1.2 mM DHP in 0.02 M Tris, pH 7.8, at 23 $^{\circ}C$; graph b, viologen dependence for triplet deactivation, measured at 830 nm, with 10 μM $Zn(TMPyP)^{4+}$, 6.1 mM DHP in 0.05 M Tris, pH 7.8, at 23 $^{\circ}C$.

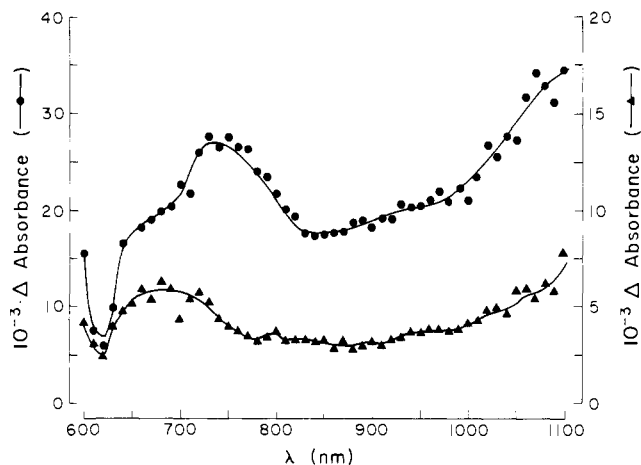


Figure 6. Spectra of $Zn(TMPyP)^{4+}$ - $C_{14}MV^{2+}$ -DHP photoexcitation intermediates. End-of-pulse spectra for the composite of self-quenched $Zn(TMPyP)^{4+}$ triplet and $C_{14}MV^{2+}$ quenched π -ion (circles) and for the $C_{14}MV^{2+}$ quenched triplet (triangles) calculated from transient spectra at 1.0 and 16 μs after excitation. Reaction conditions: 20 μM $Zn(TMPyP)^{4+}$, 0.5 mM $C_{14}MV^{2+}$, 2.4 mM DHP in 0.02 M Tris, pH 7.8, at 23 $^{\circ}C$.

chromophore, giving rise to the 740-nm absorption band, i.e., the π -anion. Oxidative quenching could not be confirmed by direct optical detection of transitory $C_{14}MV^+$ radical cation formation at 610 nm because the amplitudinal response was too low. Similarly, although net absorption was seen at 600–700 nm following laser flash excitation and relaxation in solutions containing the donor amine, TEOA, it was not possible to conclusively identify the absorbing species as $C_{14}MV^+$ ion, as opposed to reduced sensitizer or other degradation products.

The $Zn(TPPS)^{4-}$ triplet ion undergoes one-electron oxidation by DHP-bound viologens. Transitory viologen radical cation formation is clearly visible at 600 nm (Figure 7); in the absence of electron donors, the regenerative back-electron-transfer reaction occurs quantitatively by a second-order pathway. Concentration dependencies for quenching fitted the Stern-Volmer rate law: for MV^{2+} , $k_Q = 2.5 \times 10^9 M^{-1} s^{-1}$, and for $C_{14}MV^{2+}$, $k_Q = 2.4 \times 10^8 M^{-1} s^{-1}$ in 0.02 M Tris, pH 7.8, at 23 $^{\circ}C$. These reactions are remarkable because photoinitiated charge separation is virtually precluded in homogeneous solution by strong ion association of $Zn(TPPS)^{4-}$ and MV^{2+} .²⁸ This complexation, which is easily detected by bathochromic shifts in the $Zn(TPPS)^{4-}$ optical spectrum, leads to static quenching of the $Zn(II)$ porphyrin triplet. The anionic vesicle, by preferentially binding the viologen, prevents its association with the sensitizer and thereby stabilizes the electron-transfer products. Partitioning of viologens between vesicle and sensitizer can be measured from the magnitude of decrease in initially formed $Zn(TPPS)^{4-}$ triplet ion that accompanies addition of increasing amounts of viologen. At the highest

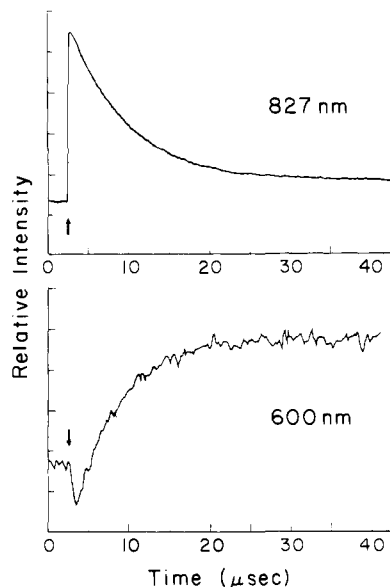


Figure 7. Oxidative quenching of photoexcited $Zn(TPPS)^{4-}$ by DHP-bound MV^{2+} . Upper trace, triplet formation and deactivation; lower trace, viologen radical formation. The arrows indicate the point of initiation of the laser pulse; amplitudes are 1 mV/division. Conditions: 20 μM $Zn(TPPS)^{4-}$, 70 μM MV^{2+} , 3.6 mM DHP in 0.02 M Tris, pH 7.8, at 23 $^{\circ}C$.

MV^{2+} concentration studied (0.2 mM), initial triplet amplitudes had decreased only about 10%, indicating nearly complete binding to DHP, whereas for $C_{14}MV^{2+}$ at the same concentration, $Zn(TPPS)^{4-}$ triplet formation was 50% sterically quenched and reached 75% by total addition of 0.6 mM $C_{14}MV^{2+}$ ion. This ordering is surprising since we had thought that the tetradecyl substituent would strengthen vesicle binding.³⁹ Presumably, $Zn(TPPS)^{4-}$ binding is enhanced to an even greater degree. The 10-fold lower quenching rate measured for $C_{14}MV^{2+}$ -DHP than for MV^{2+} -DHP suggests binding in an environment less accessible to the anionic porphyrin. Incorporation of the alkyl chain into the bilayer could orient the viologen head group more deeply within the anionic interfacial layer.

Qualitatively similar quenching behavior is seen in reactions of photosensitized $Zn(TMPyP)^{4+}$ ion with $C_{16}MV^{2+}$ adsorbed onto lecithin vesicles. Viologen radical formation occurs coincidentally with $Zn(II)$ porphyrin triplet deactivation and then subsequently decays in the absence of donors, completing the redox cycle. However, kinetic complexity is evident from the rate behavior. Triplet-state quenching is not strictly first order, and back electron transfer also deviates from strictly second-order kinetics. Moreover, rate constants calculated from best-fit plots of the integrated rate laws vary randomly from preparation to preparation, and deactivation rates also appear to increase with the degree of $C_{16}MV^{2+}$ liposomal binding. The molecular basis for this rate behavior is uncertain. It is not possible to identify concurrent reaction pathways from the kinetic plots as was done for the DHP vesicular system. Light-scattering measurements reveal that the liposomes are relatively heterogeneous,¹² suggesting that the curvature might be a consequence of differing reactivities of viologens located in different microenvironments. Others have attributed nonlinear behavior in oxidative quenching of $Zn(TMPyP)^{4+}$ in homogeneous solution to instability of the $Zn(TMPyP)^{5+}$ ion⁴⁰ and oxidative quenching of liposome-bound chlorophyll to diffusive effects arising from the high apparent viscosity of the vesicles,⁴¹ although these rationalizations do not appear to be pertinent to our studies.

(39) Brugger, P.-A.; Infelta, P. P.; Braun, A. M.; Grätzel, M. *J. Am. Chem. Soc.* **1981**, *103*, 320–326.

(40) Harriman, A.; Porter, G.; Walters, P. J. *Photochem.* **1982**, *19*, 183–187.

(41) Hurley, J. K.; Castelli, F.; Tollin, G. *Photochem. Photobiol.* **1980**, *32*, 79–86.

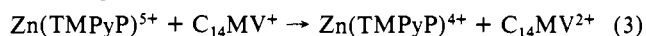
A bimolecular constant, $k_Q \approx 9 \times 10^5 \text{ M}^{-1} \text{ s}^{-1}$ (0.05 M phosphate, pH 6.5, 23 °C) was calculated for $\text{C}_{16}\text{MV}^{2+}$ -liposome oxidation of the $\text{Zn}(\text{TMPyP})^{4+}$ triplet ion from best-fit plots of the first-order decay curves. As discussed above, scatter of individual data points was high; the correlation coefficient from linear regression analysis was $r = 0.88$. Oxidative quenching of $\text{Zn}(\text{TMPyP})^{4+}$ by viologen bound to a formally uncharged, zwitterionic vesicle surface is several orders of magnitude slower than $\text{Zn}(\text{TPPS})^{4+}$ quenching by viologen bound to an anionic surface. Similar differences measured for MV^{2+} quenching of the $\text{Zn}(\text{II})$ porphyrin triplet ions in homogeneous solution have been attributed to the greater ease of $\text{Zn}(\text{TPPS})^{4+}$ ion oxidation.²⁸ The predominance of energetic factors in controlling reactivities of vesicle-bound viologens over electrostatic forces suggests that electron transfer is long range in character. Several clear precedents exist for this claim in the redox photochemistry of metalloporphyrins^{34,35} and other metal ions.⁴²

Mechanisms of Zinc(II) Porphyrin Deactivation. The rapid deactivation of DHP-bound $\text{Zn}(\text{TMPyP})^{4+}$ triplet ion is undoubtedly caused by interaction with neighboring $\text{Zn}(\text{II})$ porphyrins. Self-quenching has been reported for several metalloporphyrins and chlorins in concentrated solutions³⁰ and adsorbed at various interfaces.⁸ Concentration quenching by ground-state molecules is relatively inefficient in homogeneous solution but may be the deactivation mechanism in DHP vesicles since no evidence for T-T annihilation was obtained from the laser flash intensity studies. The theory of encounter-controlled reactions between donor-acceptor pairs constrained to spherical surfaces has been developed⁴³ and shown to account for ion dismutation kinetics on micellar surfaces⁴⁴ and for chlorophyll *a* cation recombination with quinone radical anion in liposomes.⁴⁵ The model may not be applicable in the present case, however. Given a $\text{Zn}(\text{TMPyP})^{4+}$ triplet ion lifetime, $\tau = 2 \times 10^{-4} \text{ s}$, and assuming the surface viscosity determined from the micellar kinetics, $\eta \approx 15 \text{ cP}$, we calculate a mean square displacement for zinc(II) porphyrin during its triplet lifetime of $(\Delta \bar{X}^2)^{1/2} = 1.4 \times 10^3 \text{ \AA}$, far greater than the average separation of $\text{Zn}(\text{II})$ porphyrins under our experimental conditions (Table I). Unless surface diffusion of the $\text{Zn}(\text{TMPyP})^{4+}$ ion is anomalously low, multiple collisions will occur within its triplet lifetime. Because a substantial fraction of the triplet ion decays by simple first-order kinetics (Table I, the k_3 pathway), collisional quenching cannot be encounter limited under these circumstances. If quenching requires activation, then conceptually the reaction rate should depend upon the number of collisions in unit time and space, analogous to homogeneous solution. Consequently, measured deactivation rate constants should exhibit dependence upon the surface concentration of $\text{Zn}(\text{TMPyP})^{4+}$ ions. The measured rate constant is nearly concentration independent, however (Table I). An alternative model has been proposed by Cellarius and Mauzerall, based upon their observation that fluorescence quenching in pheophytin bound to polystyrene particles occurs well before perturbation of its optical spectrum or loss of photosensitized dye oxidation.⁴⁶ This behavior is attributed to the simultaneous presence of two general types of aggregates, one of which has an absorption spectrum identical to the monomer. The presence of similar optically undetectable aggregates on DHP could account for the rapid deactivation pathways, in particular its observed first-order character and increase in relative contribution with increasing surface coverage (Table I). Distinguishing between the alternatives of "slow" $\text{Zn}(\text{TMPyP})^{4+}$ diffusion and aggregate formation will require additional physical characterization of the vesicle-bound porphyrins.

Mobilities must be considerably less for precursors to the π -cation and π -anion pairs formed by electron-transfer quenching since the precursor lifetimes are relatively short. For $\tau < 10^{-8} \text{ s}$, we calculate $(\Delta \bar{X}^2)^{1/2} < 8 \text{ \AA}$, i.e., less than the length of the porphyrin major axis. Photoinitiated electron transfer can occur over porphyrin internuclear separation distances as large as about 20 \AA .^{34,35} Ionogenesis in DHP-bound vesicles can therefore occur only between ions that are separated by a center-to-center distance less than $\sim 40 \text{ \AA}$ at the time of initiation of the laser flash. The number of ions within this distance should decrease markedly with dilution over the experimental range of $[\text{DHP}]/[\text{P}]$ ratios used in this study, assuming a random distribution of zinc(II) porphyrin; it is therefore surprising that the ion yields are found to be nearly invariant (Table I). The data again suggest nonrandom distribution, i.e., aggregation.

The rate constant measured for $\text{Zn}(\text{TMPyP})^{3+}$ π -anion quenching by $\text{C}_{14}\text{MV}^{2+}$ (eq 2) in DHP vesicle suspensions, $k_Q = \text{Zn}(\text{TMPyP})^{3+} + \text{C}_{14}\text{MV}^{2+} \rightarrow \text{Zn}(\text{TMPyP})^{4+} + \text{C}_{14}\text{MV}^+$ (2) $1.7 \times 10^9 \text{ M}^{-1} \text{ s}^{-1}$, is several orders of magnitude larger than can be accounted for by surface diffusional reactions,⁴³ indicating that one of the reactants is no longer vesicle bound. Since all criteria indicate that the alkylviologen is strongly bound, formation of the π -anion must be followed by its release from the vesicle surface. This conclusion seems reasonable, given that the increased electron density resides on the porphyrin periphery where it will encounter charge repulsion by the anionic vesicle head groups.⁴⁷ The kinetic argument is supported by the nearly identical quenching rate constants for oxidation of unbound $\text{Zn}(\text{TPPS})^{4+}$ triplet ions by DHP bound viologens and, to a lesser extent, of unbound $\text{Zn}(\text{TMPyP})^{4+}$ triplet ions by lecithin-bound $\text{C}_{16}\text{MV}^{2+}$. Expulsion of $\text{Zn}(\text{TMPyP})^{3+}$ from the vesicle also provides an explanation of the longevity of the charge-separated ions. Without escape, back electron transfer in the geminate redox pair would be expected to be rapid, giving rise to first-order quenching.⁴³

Accumulation of viologen radical cation is not seen in the transient spectra of the oxidatively quenched ion (Figure 6), indicating that its reaction with the π -cation, i.e.,



must also be rapid. Consistent with this proposal, reaction 3 is exothermic by about 38 kcal/mol, based upon standard electrochemical potentials.⁴⁸ Since both reactant ions are probably vesicle bound, their minimal lifetime, assuming encounter-controlled reaction, is of the order of a few microseconds.⁴³ In this regard, the weak maximum appearing at 690 nm in the calculated end-of-pulse triplet spectrum (Figure 6) might arise from yet unquenched π -cations. Similarly, if $\text{Zn}(\text{TMPyP})^{3+}$ ion is released, the porphyrin redox pair becomes statistically decorrelated and the back reaction between π -cation and π -anion is second order. The weak maximum in the "slow" triplet spectrum obtained in the absence of added quenchers (Figure 4) can be attributed to surviving $\text{Zn}(\text{TMPyP})^{5+}$ and $\text{Zn}(\text{TMPyP})^{3+}$ ions that have not been corrected for upon assuming first-order kinetics in the data analysis. The rate constant necessary to account for the second-order back reaction, $k \approx 10^{11} \text{ M}^{-1} \text{ s}^{-1}$, is somewhat larger than the usual encounter-controlled limit, suggesting that the reaction cross-section is larger than the ionic radii of the reactant ions. More detailed analysis is hampered by the lack of information on effective charges and dielectric strength at the DHP-solution interface.

The slow first-order decay of the DHP-bound $\text{Zn}(\text{II})$ porphyrin triplet in DHP-containing solutions proceeds at a rate nearly

(42) Norton, K. A.; Hurst, J. K. *J. Am. Chem. Soc.* **1982**, *104*, 5960-5966.

(43) Hatlee, M. D.; Kozak, J. J.; Rothenberger, G.; Infelta, P. P.; Grätzel, M. *J. Phys. Chem.* **1980**, *84*, 1508-1519.

(44) Frank, A. J.; Grätzel, M.; Kozak, J. J. *J. Am. Chem. Soc.* **1976**, *98*, 3317-3321; Henglein, A.; Proske, T. *Ber. Bunsenges. Phys. Chem.* **1978**, *82*, 471-476.

(45) Hurley, J. K.; Castelli, F.; Tollin, G. *Photochem. Photobiol.* **1981**, *34*, 623-631.

(46) Cellarius, R. A.; Mauzerall, D. *Biochim. Biophys. Acta* **1966**, *112*, 235-255.

(47) Indirect evidence consistent with this interpretation is found in the redox behavior of solutions containing DHP bound $\text{C}_{14}\text{MV}^{2+}$, $\text{Zn}(\text{TPPS})^{4+}$, and the relatively effective donor, EDTA. Continuous illumination of this system gives rise to nearly complete porphyrin bleaching over a period of ~ 75 min without detectable formation of C_{14}MV^+ ion. Thus, despite facile oxidative quenching of $^3(\text{Zn}(\text{TPPS})^{4+})$ by $\text{C}_{14}\text{MV}^{2+}$ -DHP, the $\text{Zn}(\text{TPPS})^{5+}$ π -anion is incapable of reacting with the vesicle bound viologen at a rate that is competitive with its own disproportionation.

(48) Hornbaugh, W. A.; Sundquist, J. E.; Bunis, R. H.; Orme-Johnson, W. H. *Biochemistry* **1976**, *15*, 2633-2641.

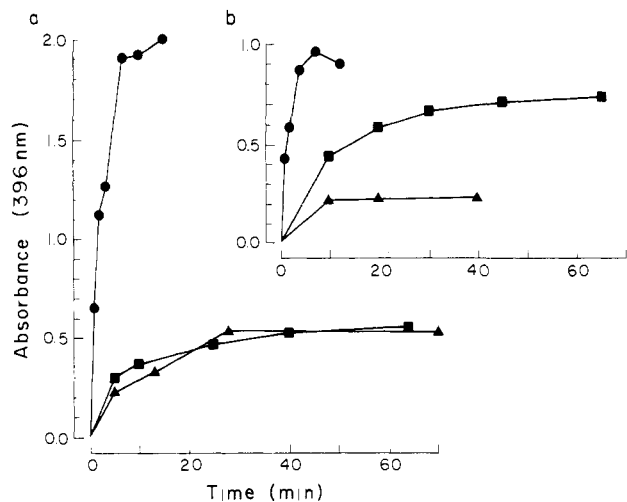
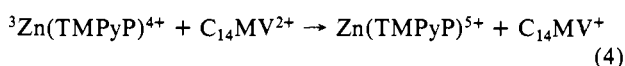


Figure 8. Zn(TMPyP)⁴⁺ photosensitized viologen reduction. Graph a: MV⁺ formation; (circles) 10 μM Zn(TMPyP)⁴⁺, 0.24 mM MV²⁺, DHP absent; (squares) 10 μM Zn(TMPyP)⁴⁺, 1.2 mM MV²⁺, 6 mM DHP, $r = 600$; (triangles) 20 μM Zn(TMPyP)⁴⁺, 0.24 mM MV²⁺, 1.2 mM DHP, $r = 60$. Graph b: C₁₄MV⁺ formation; (circles) 10 μM Zn(TMPyP)⁴⁺, 0.21 mM C₁₄MV²⁺, DHP absent; (squares) 10 μM Zn(TMPyP)⁴⁺, 1.2 mM C₁₄MV²⁺, 6 mM DHP; (triangles) 20 μM Zn(TMPyP)⁴⁺, 0.24 mM C₁₄MV²⁺, 1.2 mM DHP. All reactions in 0.02 M TEOA, pH 7.8, at ambient temperature.

identical with its decay in homogeneous solution,^{28,29} suggesting very similar deexcitation mechanisms exist in the two environments. Two observations indicate that the pathway is not due to unbound Zn(TMPyP)⁴⁺ ion. First, the fractional reaction by this pathway increases with increasing [DHP]/[P] ratios (Table I), rather than decreasing; assuming no cooperative interaction, the fraction of unbound porphyrin decreases with an increasing proportion of DHP so that the opposite behavior would be expected for unbound sensitizer. Second, oxidative quenching by C₁₄MV²⁺, i.e.,



does not follow Stern–Volmer kinetics (Figure 5), as would also be expected for unbound sensitizer. The absence of measurable dependence upon quencher concentration at high C₁₄MV²⁺ concentration levels suggests that a rate-limiting barrier to free diffusion along the vesicle surface may exist. The lack of identifiable C₁₄MV⁺ formation in laser flash studies of sensitizer and C₁₄MV²⁺ bound vesicles in the presence of TEOA indicates that the donor amine competes poorly with the alkylviologen radicals for Zn(TMPyP)⁵⁺ π-cations formed in reactions 1 and 4, leading to low net accumulation of redox products. These effects are also seen in continuous photolysis experiments where both the rate and extent of viologen production are reduced with inclusion of DHP vesicles in the reaction cell (Figure 8). Reduced C₁₄MV⁺ formation rates and yields at higher surface concentration levels of Zn(TMPyP)⁴⁺ may reflect the proportionately greater contribution from the rapid triplet self-quenching pathway, although this effect is less pronounced for systems containing MV²⁺ ion.

Transmembrane Redox Reactions. Several reports of photosensitized oxidation–reduction across vesicle bilayers have recently appeared.^{3–6,49} Although the spatial organization and chemical composition of these vesicle assemblies vary, in each instance the photosensitizer is vesicle bound. The molecular mechanisms that have been proposed^{3,6} involve rate-limiting electron tunneling across the hydrocarbon barrier. We have recently presented evidence that in one of these systems, DHP vesicles containing sensitizer and MV²⁺ ions on outer and inner surfaces, respectively, with a sacrificial donor in the external medium, net redox occurs by photostimulated *diffusion* of viologen across the bilayer followed

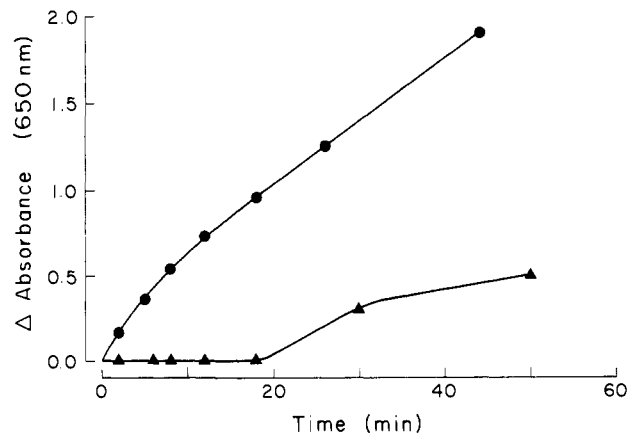


Figure 9. Zn(TPPS)⁴⁻ photosensitized C₁₆MV²⁺–DHP reduction. Circles, continuous illumination of 88 μM Zn(TPPS)⁴⁻ in 0.1 M tricine, pH 7.2, with 0.58 mM C₁₆MV²⁺ bound to inner and outer surfaces of 3.3 mM DHP; triangles, same conditions except vesicles contain ~1 mM Fe(CN)₆³⁻ within their inner aqueous phase.²⁴

Table II. Initial Rates of Zn(TPPS)⁴⁻ Sensitized C₁₆MV⁺ Formation^a

vesicle configuration ^b	R _i , nM s ⁻¹ c	E _a , kcal/mol ^d
C ₁₆ MV ²⁺ /DHP/C ₁₆ MV ²⁺ , Zn(TPPS) ⁴⁻	6.2	6.6
/DHP/C ₁₆ MV ²⁺ , Zn(TPPS) ⁴⁻	6.2	8.3
Fe(CN) ₆ ³⁻ /DHP/C ₁₆ MV ²⁺ , Zn(TPPS) ⁴⁻	46	
Fe(CN) ₆ ³⁻ , C ₁₆ MV ²⁺ /DHP/C ₁₆ MV ²⁺ , Zn(TPPS) ⁴⁻	2.2 ^e	15
C ₁₆ MV ²⁺ /DHP/C ₁₆ MV ²⁺ , Fe(CN) ₆ ³⁻ , Zn(TPPS) ⁴⁻	0	

^a In 0.02 M Tris, 0.1 M tricine, pH 7.8, with [Zn(TPPS)⁴⁻] = 40 μM, [C₁₆MV²⁺] = 0.2 μM, [DHP] = 4 mM, internal [Fe(CN)₆³⁻] ≈ 1 mM, when present;²⁴ illumination conditions given in the text. ^b Notation is (inner aqueous phase)/(vesicle)/(external aqueous phase). ^c At 23 °C, determined by absorbance increases at 600 nm. ^d 10–30 °C. ^e After 10–35-min induction period.

by oxidative quenching of photoexcited sensitizer by externally bound MV²⁺.⁷ In support of this interpretation, the triphasic decay curves of externally bound photoexcited Zn(TMPyP)⁴⁺ are unaffected by the presence of MV²⁺ ion on the inner surface. Thus, no evidence for transmembrane oxidative quenching is found in the transient kinetic behavior of the asymmetrically organized DHP vesicles. Since the phenomenon of photostimulated diffusion might prove to be quite general, our results cast doubt on claims for transmembrane electron tunneling in the other systems as well.

With Zn(TPPS)⁴⁻ photosensitized oxidation of DHP-bound viologens, photostimulated diffusion leading to mixing of initially compartmented reagents is not a problem since the sensitizer does not adsorb to the vesicle. Illumination of Zn(TPPS)⁴⁻ in 0.1 M tricine, pH 7–8, in the presence of C₁₆MV²⁺–DHP vesicle suspensions gives immediate, rapid formation of monomeric viologen radical cation. If the vesicles also contain Fe(CN)₆³⁻ ion within their internal aqueous phase, then C₁₆MV⁺ formation occurs much more slowly and its appearance is preceded by a pronounced induction period (Figure 9). The amount of viologen radical that would be formed during the induction period if Fe(CN)₆³⁻ were absent can be calculated from the measured initial formation rates for the other systems (Table II). Within a large experimental uncertainty, the calculated values coincide with the amount of occluded Fe(CN)₆³⁻ ion, suggesting that induction can be attributed to ferricyanide oxidation of the reduced viologen radical.⁵⁰

(50) When solutions contain 5–50 μM Fe(CN)₆³⁻ in the external medium, no radical accumulates within a 60-min illumination period. Ferricyanide oxidation of MV⁺ ion is encounter controlled in homogeneous solution;⁵¹ despite the unfavorable electrostatics, rapid reaction can also be expected with DHP-bound C₁₆MV⁺ ion.

(51) Oliveira, L. A. A.; Haim, A. J. Am. Chem. Soc. 1982, 104, 3363–3366.

(49) Tunuli, M. S.; Fendler, J. H. J. Am. Chem. Soc. 1981, 103, 2507–2513.

Since, as discussed above, $\text{Fe}(\text{CN})_6^{3-}$ does not diffuse across the vesicle membrane over the time course of these studies, the rate behavior implies net transmembrane redox involving the bound viologens. Reaction mechanisms could involve either transmembrane diffusion of C_{16}MV^+ from the outer to inner surface or transmembrane electron exchange between external C_{16}MV^+ and internal $\text{C}_{16}\text{MV}^{2+}$ ions, followed by radical scavenging by $\text{Fe}(\text{CN})_6^{3-}$ on the inner surface. Asymmetrically organized vesicles with $\text{C}_{16}\text{MV}^{2+}$ only bound to their outer surfaces and carrying internalized $\text{Fe}(\text{CN})_6^{3-}$ showed immediate formation of viologen radical, i.e., no induction, with a 5-fold rate enhancement over the photosensitized reaction in absence of $\text{Fe}(\text{CN})_6^{3-}$. Thus, the transmembrane reaction requires $\text{C}_{16}\text{MV}^{2+}$ on both surfaces, an observation that is most simply interpreted in terms of transmembrane electron exchange between the viologen mono- and dications. Rate parameters determined from initial slopes of absorbance vs. time plots for $\text{C}_{16}\text{MV}^{2+}$ reduction in various vesicle configurations are listed in Table II. Studies are continuing to identify the transmembrane oxidation-reduction mechanism.

Concluding Remarks

Adsorption of $\text{Zn}(\text{TMPyP})^{4+}$ ion onto DHP vesicles generates a multiplicity of deactivation pathways for the photoexcited ion. Three predominant pathways involving self-quenching, ionogenesis, and "spontaneous" decay have been identified from observation of the kinetic and optical absorption properties of the transient species and their reactivities toward alkylviologens. Although this mechanistic diversity implies the existence of molecular organizes at the vesicle interface, we could find no evidence for aggregation using absorption spectrophotometric methods. The rapid formation of $\text{Zn}(\text{II})$ porphyrin π -ions is particularly noteworthy since they may arise by oxidation-reduction involving singlet photoexcited ions. In this sense, the reaction may mimic photosynthetic redox centers, for which charge separation is initiated from photoexcited singlet states.^{52,53} *In vitro* models exhibiting detectable charge pair formation emanating from the singlet state are rare; most examples are covalently linked photoredox pairs that meet special spatial and orientational geometric requirements.⁵⁴

The inefficient formation of redox products by oxidative quenching when both $\text{Zn}(\text{TMPyP})^{4+}$ and acceptor viologens are

adsorbed to the vesicle is a consequence of a relatively slow reaction between bound reactants (eq 4), rapid cyclic back electron transfer from π -anion to π -cation using viologen as the relay (eq 2, 3), and, at higher surface concentrations, competitive self-quenching of the sensitizer triplet ion. The relative rates can be rationalized by assuming that the monopositively charged viologen radicals have relatively large mobilities on the vesicle surface, presumably because electrostatic forces are considerably less than for the other ions. This might be interpreted as weaker Coulombic attraction or binding at a single surface site, as opposed to formation of two and four distinct electrostatic bonds upon adsorption of C_nMV^{2+} and $\text{Zn}(\text{TMPyP})^{4+}$ ions, respectively. Since the diffusional barrier for $\text{Zn}(\text{TMPyP})^{3+}$ ion is overcome by its release from DHP, both reactions 2 and 3 involve relatively mobile species whereas reaction 4 does not.

Regardless of mechanistic interpretations, it is evident that vesicles and liposomal suspensions are capable of dramatically altering the solution photochemistry of $\text{Zn}(\text{II})$ porphyrins. The most useful observation from the standpoint of photoconversion is that selective adsorption of viologens to DHP provides a means for overcoming static quenching that otherwise occurs by $\text{Zn}(\text{TPPS})^+-\text{C}_n\text{MV}^{2+}$ ion pair formation and severely limits net redox in homogeneous solution. Use of DHP in this instance is particularly effective because the electrostatic barrier imposed by the anionic vesicle surface to electron transfer across the aqueous-vesicle interface is small (e.g., k_Q for oxidative quenching of $^3(\text{Zn}(\text{TPPS})^+)$ by MV^{2+} and MV^{2+} -DHP are $1.4 \times 10^{10} \text{ M}^{-1} \text{ s}^{-1}$ (ref 28) and $2.5 \times 10^9 \text{ M}^{-1} \text{ s}^{-1}$, respectively). In general, since bound viologen appears to act as a transmembrane charge relay and $\text{Zn}(\text{TMPyP})^{4+}$ binding leads to its own destabilization, systems containing $\text{Zn}(\text{II})$ porphyrins in solution with membrane-bound acceptors will be more practicable than other spatial configurations in application to photocatalytic devices that rely upon generation of membrane separated redox products.

Acknowledgment. J.K.H. and L.Y.C.L. express their gratitude to Drs. André M. Braun and Kuppuswamy Kalyanasundaram, EPFL, for their generous gifts of experimental materials, to Drs. Robin Humphry-Baker, Pierre P. Infelta, and Keith Monserrat, EPFL, for instruction and advice on experimental methodology, and to Dr. Yves-M. Tricot, CSIRO, for communicating results prior to publication. Financial support was provided by the Oregon Graduate Center through the auspices of its faculty sabbatical leave program and by NIH through a grant (GM 20943) to J.K.H.

Registry No. $\text{Zn}(\text{TMPyP})^{4+}$, 40603-58-5; $\text{Zn}(\text{TPPS})^+$, 80004-36-0; $\text{C}_{14}\text{MV}^{2+}$, 79039-57-9; $\text{C}_{16}\text{MV}^{2+}$, 77814-50-7; MV^{2+} , 4685-14-7; $\text{Fe}(\text{CN})_6^{3-}$, 13408-62-3; DHP, 2197-63-9.

(52) Shuvalov, V. A.; Parson, W. W. *Proc. Natl. Acad. Sci. U.S.A.* **1981**, *78*, 957-961, and references therein.

(53) Shuvalov, V. A.; Klevanik, A. V.; Sharkov, A. V.; Kryukov, P. G.; Ke, B. *FEBS Lett.* **1979**, *107*, 313-316.

(54) Connolly, J. S. In "Photochemical Conversion and Storage of Solar Energy—1982", Part A; Rabani, J., Ed.; Weizmann Science Press of Israel: 1982; pp 175-204, and references therein.

The Absence of Bonding Electron Density in Certain Covalent Bonds As Revealed by X-ray Analysis

Jack D. Dunitz* and Paul Seiler

Contribution from the Organic Chemistry Laboratory of the Swiss Federal Institute of Technology, CH-8092 Zürich, Switzerland. Received May 18, 1983

Abstract: Electron-density difference maps obtained from an accurate low-temperature X-ray analysis of 1,2,7,8-tetraaza-4,5,10,11-tetraoxatricyclo[6.4.1.1^{2,7}] tetradecane (**1**) show a density deficit at the center of the O-O bond and only weak density accumulations at the centers of the C-O and N-N bonds. Peaks corresponding to tetrahedrally oriented lone pairs are observed at the N and O atoms. These findings and others indicate that accumulation of charge (bonding density) in the internuclear region as occurs in the hydrogen molecule may not be characteristic of covalent bonds in general.

Because of its relative simplicity, the H_2 molecule is generally taken as the paradigm of the covalent bond,¹ and one of its cardinal

features, the accumulation of negative charge between the nuclei, seems to have established itself as the standard textbook expla-